

• Measurements in transients under separated flow conditions. Some measurements of this type are being done using a six Pitot tube "rake" in a large pipe.

ACKNOWLEDGMENT

We would like to thank the Idaho National Engineering Laboratory, Idaho Falls, and Atomic Energy of Canada, Pinawa, Manitoba, for supporting this work. We would also like to acknowledge the assistance provided by Martin Vandebroek during the experiments.

NOTATION

C_1, C_2 = constants, defined by Eqs. 14 and 15, respectively
 G_2, G_4, G_6, G_7 = local mass flux at 0.286 diameter above the center of the pipe, at the center, at 0.286 and 0.429 diameter below the center, respectively
 G'_6 = local mass flux, defined by Eq. 15
 G_{ij} = local mass flux at location ij
 \bar{G} = cross-section averaged mass flux
 I_x = measured gamma intensity
 I_l, I_g = intensities measured for the cases of the tube full of liquid and gas, respectively
 P_{ij} = fraction of area of the j th square in which it is intersected by the i th ray
 $\Delta p_{ij}(t)$ = instantaneous differential pressure of the impact head at position ij
 R_i = chordal liquid fraction at i th chord
 V = velocity
 V^a = variance, defined by Eq. 12
 W_j = local liquid fraction at position j
 \bar{W} = cross-section averaged liquid fraction
 α_{ij}, α_j = local void fraction at position ij and j , respectively
 $\bar{\alpha}_i$ = chordal void fraction at i th chord
 ρ = density
 $\rho_{ij}(t)$ = the instantaneous local fluid density at position ij
 $\langle \rangle$ = time mean value

Subscript

g = gas phase
 l = liquid phase
 m = mixture

LITERATURE CITED

- Anderson, G. H., and B. G. Mantzouranis, "Two-Phase (Gas/Liquid) Flow Phenomena—II Liquid Entrainment," *Chem. Eng. Sci.*, **12**, 233 (1960).
 Banerjee, S., and D. M. Nguyen, "Mass Velocity Measurement in Steam-Water Flow by Pitot Tubes," *AIChE J.*, **23**, 385 (1977).
 Banerjee, S., T. R. Heidrick, and E. Rhodes, "Development and Calibration of Instruments in Transient Two-Phase Flow," Proceedings of the OECD/CSNI Specialists Meeting on *Transient Two-Phase Flow*, Paris, France (June, 1978).
 Banerjee, S., and R. T. Lahey, "Advances in Two-Phase Flow Instrumentation," *Advances in Nuclear Sci. and Tech.*, (1980, in press).
 Brockett, G. F., and R. T. Johnson, "Single Phase and Two-Phase Flow Measurement Techniques for Reactor Safety Studies," Electric Power Research Institute Report, *EPRI-ND-195* (1976).
 Delhaye, J. M., "Two-Phase Flow Measurements," *Bull. D'Inform. Sci. Tech.*, **197**, S-20 (1963).
 Gordon, R., R. Bender, and G. T. Herman, "Algebraic Reconstruction Technique (ART) for Three-Dimensional Electron Microscopy and X-Ray Photography," *J. Theor. Biol.*, **29**, 471 (1970).
 Heidrick, T. R., J. R. Saltvold, and S. Banerjee, "Application of a 3-Beam γ -Densitometer to Two-Phase Flow Regime and Density Measurements," *AIChE Symposium Series*, **73**, No. 164, 248 (1978).
 Heidrick, T. R., J. R. Saltvold, S. Banerjee, and D. Nguyen, "Cross-Section Averaged Density and Mass Flux Measurements in Two-Phase Flow Through Pipes," *Measurements in Polyphase Flow*, ASME, 1-10 (1978).
 Herman, G. T., A. Lent, and S. W. Rowland, "ART: Mathematics and Applications," *J. Theor. Biol.*, **42**, 1 (1973).
 Hewitt, G. F., and P. C. Lovegrove, "Experimental Methods in Two-Phase Flow Studies," Electric Power Research Institute Report, *EPRI NP-118* (1976).
 Petrick, M., and B. S. Swanson, "Radiation Attenuation Method of Measuring Density of a Two-Phase Fluid," *Review of Scientific Instruments*, **29**, No. 12, 1079 (1958).
 Zakaib, G. D., A. A. Harms, and J. Vlachopoulos, "Two-Dimensional Void Reconstruction by Neutron Transmission," *Nucl. Sci. and Eng.*, **65**, 145 (1978).

Manuscript received March 10, 1980; revision received July 14, and accepted July 16, 1980.

Efficiency of Mixing from Data on Fast Reactions in Multi-Jet Reactors and Stirred Tanks

J. M. OTTINO

Department of Chemical Engineering and Materials Science
 University of Minnesota
 Minneapolis, MN 55455

Some fluid mechanical information concerning mixing generation in complex flow fields can be obtained from conversion data of fast chemical reactions. Computation of such information and averages required in the procedure are presented here. Complex turbulent flow fields present deterministic-like behavior when analyzed in average sense with regard to mixing generation.

SCOPE

Mixing with chemical reaction is a process that involves fluid mechanics, diffusion, and kinetics. In general, these three mechanisms govern reaction in any reacting mixture. Any rea-

sonable mixing description should give an emphasis to all of these processes in proportion to the importance of their effects.

The independent variable of mixing of reacting fluids without changes in physical properties is the flow field. Chemical reaction results, such as spatial distributions of conversion or selectivity, are dependent variables governed by fluid mechanical effects. It is then, in principle, possible to obtain fluid

The author is presently with Department of Chemical Engineering, University of Massachusetts, Amherst, MA 01003.

mechanical information from conversion data (e.g., Mao and Toor, 1970). Experimental data are based on *local averages*, e.g., mean concentration value in a small volume element in the neighborhood of the sensor mechanisms (e.g., the tip of a thermocouple).

Averaging implies fundamentally loss of information. A careful physical analysis must be done to account for this lost information in order to obtain a meaningful interpretation of the flow field. Analysis is based in terms of a lamellar or stretching model (Ottino *et al.*, 1979; Ranz, 1979). This is a continuum, deterministic description based on a Lagrangian

point of view for computation of interactions between local fluid motion, diffusion, and chemical reaction. Two quantities, a_v , intermaterial area per unit volume and s , striation thickness, are defined to describe the fluid mechanical state of a system mixed or being mixed. These quantities are related to one another and to the local fluid mechanics, mass transfer, and reaction. Fluid mechanical effects are bounded by local dissipation. An efficiency function measuring the closeness to this maximum is used to quantify effectiveness of mixing flows. This is the framework for the analysis of efficiency of mixing in multi-jet reactors and stirred tanks.

CONCLUSIONS AND SIGNIFICANCE

A lamellar mixing model has been used to obtain *average* fluid mechanical information of two processes involving molecular diffusion and chemical reaction in relatively complex flow fields. Due to the nature of the reaction (fast, diffusion controlled) all local fluid mechanical independency can be absorbed in a warped time scale describing pure diffusion in striation thickness-based space. Theoretical information can then be combined with real time dependent experimental information to obtain average information of the flow field.

Assumptions and restrictions of the analysis have been indicated; loss of information due to averaging seems to be the critical point.

We have not analyzed the mechanistic description of the generated flows. We have rather shown that turbulent flows, usually regarded as chaotic, present deterministic-like behavior when analyzed in an average sense with regard to

mixing generation. Fluid mechanical information is condensed in an efficiency function whose value can be determined by fast reactions experiments. Mechanistic fluid motion models can be compared with this average description.

The construction of more accurate (or perhaps only more elaborate) methods for dealing with mixedness distributions and assumptions at micro-flow level is recognized but only the main structure is the subject here.

The ultimate aim is quantitative understanding of specificity of reactions and selectivity with respect to intermediate products in any flow field. This method of analysis leading to average fluid mechanical information through a particular known reaction can eventually be used to predict behavior of complex reactions in the same flow field. Problems in blending, chemical reactors, and combustion processes await chemical engineering analysis.

INTRODUCTION

The detailed modeling of an incompletely mixed chemical reactor, involving fluid mechanics, diffusion, and reaction, usually calls for information and parameter values which are either inaccurately known or perhaps inaccessible. With the exception of cases in which a detailed mechanistic description is possible, analysis of mixing effects should be based on proper average descriptions. These average descriptions, based on a sufficiently detailed model, should provide also information regarding the errors introduced by the averaging processes.

This paper concerns the specialization of a Lamellar Mixing Model (Ottino *et al.*, 1979; Ranz, 1979) to analysis of the fluid mechanical details of two standard types of chemical reactors: continuous flow reactors, e.g., a tubular reactor; and closed volume reactors, e.g., a stirred-tank reactor.

First the model is applied to the case of mixing turbulence produced by a multijet device in a tubular reactor. Extensive experimental information (Fisher, 1974) for fast acid-base reaction is used to obtain values of mixing efficiency and show compatibility with theoretical predictions. Secondly, the model is used to find efficiencies for mixing in stirred tanks (Fisher, 1974). Both situations involve the so-called mixing of separate reactants (Brodkey, 1966, p. 80). In the multijet reactor initial segregation is produced by a particular way of feeding the reactants while in the stirred tank it is due to initial geometrical disposition of the fluids.

In both cases, the flow field has been divided into populations of relatively simple, small scale flows called microflow elements, S_X . Materials being mixed are structured as lamellar composites characterized by a time dependent striation thickness, $s(t)$. The following scale ordering is assumed to hold:

$$s(t) \ll \text{size of } S_X \ll L \quad (1.1)$$

where L is a characteristic dimension of the system. Intermaterial area density, amount of contact area per unit volume, is introduced as a macroscopic field variable which is a point function on a macroscopic scale but where its value is determined by local averages of the actual microstructure of the system as:

$$a_r(X, t) = \frac{1}{S_X} \int_{S_X} a_r dv \quad (1.2)$$

Striation thickness in S_X is defined as:

$$s \equiv [a_r(X, t)]^{-1} \quad (1.3)$$

The objective is to demonstrate application of a Lamellar Mixing Model (Ottino *et al.*, 1979; Ranz, 1979; Ottino, 1980) to complex flow fields and to show how *average fluid mechanical information* can be obtained from chemical conversion by assuming a *particular model of reaction*.

We begin analysis with the solution of the problem of local fluid mechanics, diffusion, and reaction in *any* S_X (microflow) element for a fast reaction in *any* flow field (Ottino, 1980; Ranz, 1979). Due to the special characteristics of the reaction (very fast molecular reaction) all fluid mechanical independency can be *totally* absorbed in a warped time, τ^F . Solutions of conversions in S_X as function of warped time τ^F for this particular model are therefore applicable locally to *any* fluid mechanical situation. This is the advantage of a mathematical treatment of fast reactions based on an intermaterial frame of reference.

LAMELLAR MODELING OF FAST REACTIONS

Consider a fast-bimolecular reaction represented by:

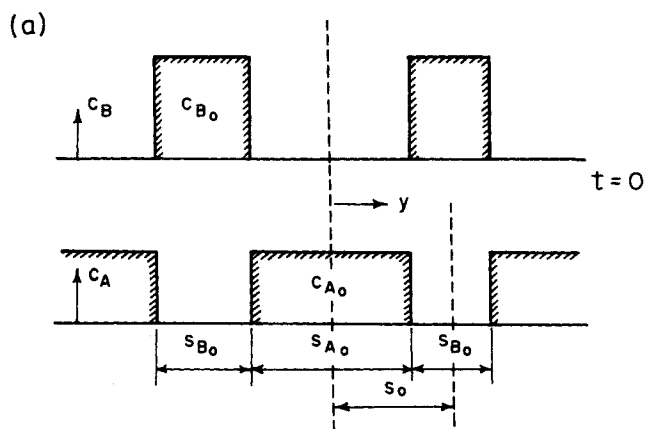


Figure 1a. Initial concentration profiles.

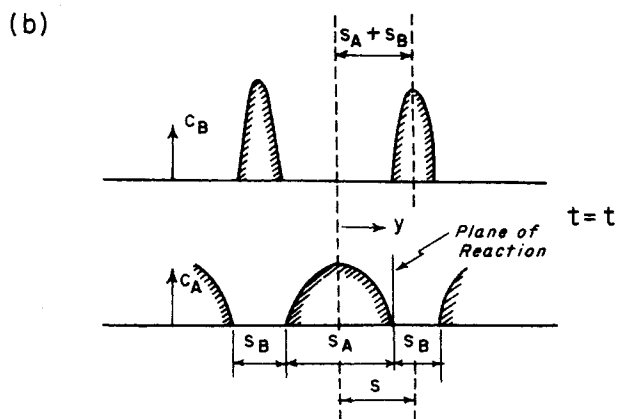
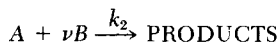


Figure 1b. Concentration profiles for very fast reactions.



with a volumetric reaction rate $r_A = -k_2 c_A c_B$. During mechanical mixing, according to the Lamellar Model, species A and B initially dissolved in a common solvent with concentrations c_{A0} and c_{B0} are found in adjacent parallel sheets with initial striation thicknesses s_{A0} and s_{B0} (Figure 1a-b). Subsequently, during motion, reaction occurs at planes separating regions containing A and B and the striation thickness, s , changes as a function of time according to (Ottino et al., 1979):

$$\frac{ds}{dt} = -\alpha(X, t)s = (\underline{D} : \hat{n}\hat{n})s \quad (2.1)$$

for S_X scales, with

$$\alpha(X, t) < \sqrt{\frac{\epsilon}{2\mu}} \quad (2.2)$$

for Newtonian fluids.

Local motion, diffusion, and reaction at S_X scales is represented by:

$$\left. \begin{aligned} \frac{\partial c_A}{\partial \tau^F} &= \frac{D_A}{(D_A + D_B)} \frac{\partial^2 c_A}{\partial \xi^2} - \left(\frac{dt}{d\tau^F} \right) k_2 c_A c_B \\ \frac{\partial c_B}{\partial \tau^F} &= \frac{D_B}{(D_A + D_B)} \frac{\partial^2 c_B}{\partial \xi^2} - \left(\frac{dt}{d\tau^F} \right) \nu k_2 c_A c_B \end{aligned} \right\} \text{ in } S_X \quad (2.3)$$

where

$$\xi = \frac{y}{s(t)} = \frac{y}{s_0} \exp \left[\int_0^t \alpha(X, t') dt' \right] \quad (2.4)$$

$$\begin{aligned} \tau^F &= \frac{(D_A + D_B)}{2s_0^2} \int_0^t \frac{1}{s^2(t')} dt' \\ &= \frac{(D_A + D_B)}{2s_0^2} \int_0^t \left[\exp 2 \int_0^{t'} \alpha(X, t'') dt'' \right] dt' \end{aligned} \quad (2.5)$$

Very fast reactions, defined as the limiting case for which coexistence of species becomes impossible, are represented by:

$$\left. \begin{aligned} \frac{\partial c_A}{\partial \tau^F} &= \frac{D_A}{(D_A + D_B)} \frac{\partial^2 c_A}{\partial \xi^2}, \quad 0 < \xi < \xi'(\tau^F) \\ \frac{\partial c_B}{\partial \tau^F} &= \frac{D_B}{(D_A + D_B)} \frac{\partial^2 c_B}{\partial \xi^2}, \quad \xi'(\tau^F) < \xi < 1 \end{aligned} \right\} \text{ in } S_X \quad (2.6)$$

coupled by a mass flux condition:

$$\nu D_A \frac{\partial c_A}{\partial \xi} \Big|_{\xi=\xi'(\tau^F)-0} = -D_B \frac{\partial c_B}{\partial \xi} \Big|_{\xi=\xi'(\tau^F)+0} \quad (2.7)$$

with an initial condition and symmetry condition ($\partial c_A / \partial \xi = 0$ at $\xi = 0$, $\partial c_B / \partial \xi = 0$ at $\xi = 1$) as shown in Figure 1.

Numerical solutions of the system (Eq. 2.6) corresponding to the initial conditions schematized in Figure 1a-b are shown in Figures 2 and 3 (Fisher, 1974; Mao and Toor, 1970). Local conversion of excess reactant F_B in nonstoichiometric cases ($F_B = F_A$ in stoichiometric cases) is represented as a function of local warped time τ^F for a variety of conditions. Figure 2 shows results

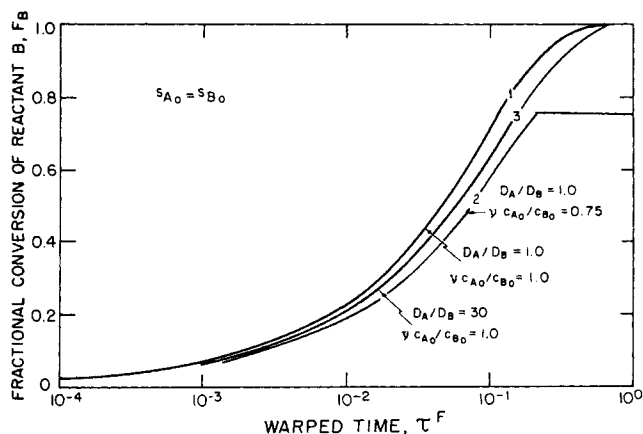


Figure 2. Extent of reaction F_B vs. τ^F (warped time) for equal striation thicknesses showing effects of different diffusion coefficients and stoichiometry (adapted from Fisher, 1974). Fractional conversion is measured with respect to the excess reactant at S_X -scales.

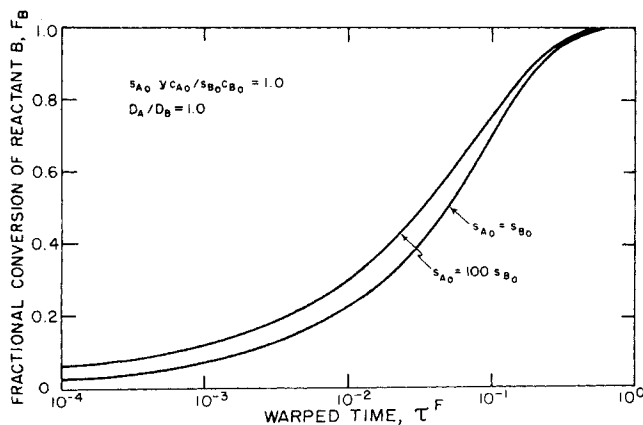


Figure 3. Extent of reaction F_B vs. τ^F (warped time) for equal diffusivities and stoichiometric amounts showing effect of unequal laminar thicknesses (adapted from Fisher, 1974).

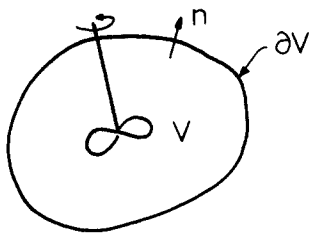


Figure 4a. Representation of a closed volume mixer.

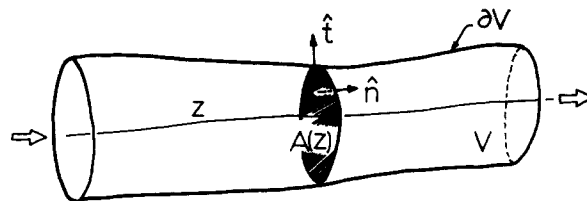


Figure 4b. Representation of a continuous flow mixer.

for several conditions in a local lamellar structure (S_X) with equal striation thicknesses. Curve 1 shows the course of reaction with equal diffusivities and stoichiometric amount of reactants at S_X scales. It forms a basis for comparison with other reaction conditions. Insufficient A limits the reaction in curve 2 while the reactant diffusivities remain equal. Curve 3 shows the effect of diffusivity variation for stoichiometrically balanced S_X -elements. Figure 3 shows the effect of distribution of striation thickness for stoichiometric condition $s_{AO} \nu_{CAO} / s_{BO} \nu_{BO} = 1$ and with $s_{AO} = 100 s_{BO}$ at S_X .

Real flows characterized by variations in local (S_X -scales) stoichiometry (represented by initial conditions) and fluid mechanical histories $[\alpha(X, t)]$ are described by some averaged form of Figures 2 and 3. These curves, so much alike, suggest that for a wide range of conditions ($D_A/D_B = 30$, $s_{AO} = 100 s_{BO}$) any local system can be represented by a single curve $F_A = F_A(\tau^F)$. The warped time (Eq. 2.5) contains only average diffusion coefficients and segregation, and local fluid mechanical history. It fails to take into account initial local variation in stoichiometry (*within* S_X) which can be introduced only in terms of initial conditions (Ottino, 1980).

APPLICATION OF LAMELLAR MIXING MODEL TO CONTINUOUS MIXERS AND CLOSED VOLUME MIXERS

The lamellar mixing model is based on a Lagrangian description of fluid mechanics, diffusion, and reaction for a general S_X -element (microflow element). However, experimental information is usually based on Eulerian averages at a fixed point or over the whole volume of the system. Some discussion is necessary on the relation of both descriptions. We propose here to specialize the ideas to continuous flow and constant volume mixers (cf. Figures 4a-b) whose fluid mechanics is discussed by Ottino et al. (1979).

Closed Volume Mixers (cf. Figure 4a)

The warped time is defined as:*

$$\tau(X, t) = D \int_0^t a_r^2(X, t') dt' \quad (3.1)$$

where X identifies an S_X element in the volume V of the mixer and t designates the associated time. The mean volumetric average of warped time and rate of increase of warped time of all the elements inside V is obtained as:

$$\bar{\tau} = D \int_0^t \bar{a}_r^2 dt' \leq D \int_0^t \bar{a}_r^2 dt' \quad (3.2)$$

$$\frac{d\bar{\tau}}{dt} = D \bar{a}_r^2 \geq D \bar{a}_r^2 \quad (3.3)$$

where $\bar{\tau}$ refers to mean volumetric values and the inequalities follow from Hölder inequality (Hardy et al., 1973). Calculation

* Coefficient D can be a combination of diffusion coefficients as in Eq. 2.5. For simplicity, a value D will be used here. Warped time τ^F will be referred to as τ .

of warped time with mean values of a_r results in an overestimation of actual warped time.

Because rate of mixing depends on rate of fluid deformation and has a maximum value for only one orientation of the intermaterial area with respect to the principle axes of deformation, rate of change of intermaterial area is given by (Ottino et al., 1979)

$$\frac{d \overline{\ln a_r}}{dt} = \overline{eff(t)} (\underline{D} : \underline{D})^{\frac{1}{2}} \quad (3.4)$$

where $\overline{eff(t)}$ is an efficiency of mixing which accounts for the history of orientation. Eq. 3.4 is more conveniently expressed by the approximation

$$\frac{d \bar{a}_r}{\bar{a}_r dt} \approx \overline{eff(t)} (\underline{D} : \underline{D})^{\frac{1}{2}} \quad (3.5)$$

considering that $\overline{\ln a_r} \leq \ln \bar{a}_r$ (Hardy et al., 1973). Function $eff(t)$ or its volumetric average $\overline{eff(t)}$ measures efficiency of mixing with respect to an upper bound given by $(\underline{D} : \underline{D})^{\frac{1}{2}}$ (Ottino et al., 1979). It is obviously less than unity. Although Eq. 3.5 is an approximation of Eq. 3.4, it is perfectly admissible to define efficiency by:

$$\frac{d \bar{a}_r}{\bar{a}_r dt} \equiv \overline{eff(t)} (\underline{D} : \underline{D})^{\frac{1}{2}}$$

This definition of efficiency is an excellent approximation to Eq. 3.5 for systems with nearly homogeneous intermaterial area distributions if distributions do not change appreciably with time.

Experimental information for closed volume mixers is usually given as mean volumetric conversion \bar{F} as function of time, $\bar{F} = \bar{F}(t)$ whereas the model is capable of predicting average conversion in the S_X -element as function of its local warped time and derivatives of warped time, $d\tau/dt$, i.e., $a_r^2(\tau)$ (cf. Eq. 2.3) so $\bar{F} = \bar{F}(\tau, d\tau/dt)$ in S_X .

Very Fast Reaction Case

Very fast reactions are described by coupled partial differential equations with matching flux condition; and conversion is solely dependent on values of warped time, i.e.,

$$\bar{F} = \bar{F}(\tau^F) \text{ in } S_X \quad (3.6)$$

If the Lamellar Mixing Model description is interpreted as one element undergoing a motion governed by mean warped time values and providing mean conversion, Eq. 3.6 is written as:

$$\bar{F} = \bar{F}(\bar{\tau}^F) \quad (3.7)$$

and combination of Eq. 3.7 and $\bar{F} = \bar{F}(t)$ produces:

$$\bar{\tau}^F = \bar{\tau}^F(t) \quad (3.8)$$

The last equation contains, by Eqs. 3.2 and 3.3, mean volumetric intermaterial area information.

Special Cases

$$(i) \quad \frac{d\bar{\tau}^F}{dt} = \text{const} \quad \text{implies that} \quad \bar{a}_v^2 = \text{const} \quad (3.9)$$

$$(ii) \quad \frac{d \ln \bar{\tau}^F}{dt} = \text{const} \quad \text{implies that} \quad \frac{\bar{d}a_v}{\bar{a}_v dt} = \frac{\text{const}}{2} \quad (3.10)$$

which by Eq. 3.5 implies, for constant $(\bar{D}:\bar{D})^\dagger$, a constant efficiency parameter

$$(iii) \quad \frac{d \ln \bar{\tau}^F}{d \ln t} = \text{const} \quad \text{implies that} \quad \frac{\bar{d}a_v}{\bar{a}_v dt} = \frac{(\text{const} - 1)}{2t} \quad (3.11)$$

which by Eq. 3.5 implies for constant $(\bar{D}:\bar{D})^\dagger$ a decaying efficiency as inverse power of time.

General Case

The general equation $F = F(\tau, d\tau/dt)$ in S_X is interpreted as:

$$\bar{F} = \bar{F}(\bar{\tau}, \bar{d}\bar{\tau}/dt) \quad \text{for } V \quad (3.12)$$

Different intermaterial area generation functions, $\bar{a}_v^2 = \bar{a}_v^2(t)$, can be used to obtain a match between Eq. 3.12 and experimental conversion data.

Continuous Flow Systems (cf. Figure 4b)

The warped time is defined as:

$$\tau(\underline{X}, t) = D \int_0^t a_v^2(\underline{X}, t') dt' \quad (3.13)$$

where \underline{X} identifies S_X elements at the entrance of the reactor and time t denotes their associated real time.

Consider a plane A at distance z at some time t (cf. Figure 4b). The elements over A will have in general different associated times and different intermaterial area values. Mean area values over plane A are:

$$\bar{\tau} = D \int_0^t \bar{a}_v^2 dt' \quad (3.14)$$

Eq. 3.14 cannot be cast as Eq. 3.2 since area average and times do not commute if the elements over A have different associated time values.

Rate of change of intermaterial area is given by (Ottino et al., 1979):

$$\frac{d \langle \ln a_v \rangle}{dz} = \frac{\overline{\text{eff}(z)}}{\bar{v}_n} \frac{(\bar{D}:\bar{D})^\dagger}{\bar{v}_n} \quad (3.15)$$

which is more conveniently expressed by the approximation:

$$\frac{d \langle \ln a_v \rangle}{\langle \ln a_v \rangle dz} \approx \frac{\overline{\text{eff}(z)}}{\bar{v}_n} \frac{(\bar{D}:\bar{D})^\dagger}{\bar{v}_n} \quad (3.16)$$

considering that $\langle \ln a_v \rangle \leq \ln \langle a_v \rangle$. [See comments after Eq. 3.5 for qualifications of $\text{eff}(z)$.]

Experimental information for continuous flow mixers is usually given as mean area conversion \bar{F} as function of distance, z , $\bar{F} = \bar{F}(z)$, whereas the Lamellar Mixing Model is capable of prediction of average conversion in the S_X -element as function of warped time and derivatives of warped time, $d\tau/dt$ (cf. Eq. 2.3) so $\bar{F} = \bar{F}(\bar{\tau}, d\bar{\tau}/dt)$ in S_X .

Very Fast Reaction Case

Conversion description in S_X is given as:

$$F = F(\tau^F)$$

which is interpreted as:

$$\bar{F} = \bar{F}(\bar{\tau}^F) \quad (3.17)$$

Combination of Eq. 3.17 and $\bar{F} = \bar{F}(z)$ produces:

$$\bar{\tau}^F = \bar{\tau}^F(z)$$

The special cases that are described here are analogous to those of the end of the previous section. Axial coordinate z and real time t are related by

$$\bar{v}_z = \frac{dz}{dt} \quad \text{or} \quad z = \int_0^t \bar{v}_z dt'$$

Limitations of the Analysis

These concepts will now be applied to analysis of experimental data. It is convenient to qualify the nature of the analysis in terms of the assumptions. First, note that fluid mechanical information is considered in an average sense. A mechanistic description of the particular flow field is the only way to avoid this loss of information. Secondly, reaction in S_X is given by a particular, assumed, model of reaction. The model, in principle, can handle the striation thickness distribution within S_X that in real flows is likely to exist. However, only initial conditions and detailed mechanistic models might provide such level of description. Complications of real flows urge averaging considerations.

We shall consider an average S_X -element with local balanced stoichiometry. Thus only curve 1 in Figure 2 is used for analysis.

The long-range diffusion problem (scales $> S_X$ -scale) is not considered. As indicated by Ottino (1980), local stoichiometry imbalance is likely to affect analysis at long times.

Distribution functions and numerical integrations might be used to study distribution effects. However, since no firm reason can be invoked for such functions, averaging analysis or detailed mechanistic descriptions is recommended here.

APPLICATION OF AN EFFICIENCY FUNCTION TO ANALYSIS OF MIXING IN MULTIJET REACTORS

Fisher in 1974 used a tubular flow reactor to study mixing with fast reactions under turbulent flow conditions. The reactor was preceded by a multijet mixing head to mix the reactants, aqueous solutions of hydrochloric acid and sodium hydroxide. Two types of mixing heads were used. The first kind was a square grid of circular holes, similar to the one used by Vassilatos and Toor (1965) but with a smaller solidity to reduce jet coalescence. The second mixing head was composed of rectangular slots. For complete details of the flow system the reader is referred to Fisher (1974).

Chemical conversion was measured by a temperature rise technique used by a number of researchers (cf. Fisher, 1974). In this method a temperature sensing device is set in the reacting solution and the temperature rise due to exothermic reaction is monitored in the adiabatic system. At any point the fractional extent of reaction is related to the measured temperature by:

$$F_A(z) = \frac{T(z) - T_o}{T_F - T_o} \quad (4.1)$$

where

$$\begin{aligned} F_A(z) &= \text{extent of reaction at position } z \\ T(z) &= \text{temperature of the reacting fluid at } z \\ T_o &= \text{mean inlet temperature of the unreacted fluid} \\ T_F &= \text{final temperature at completion of reaction} \end{aligned}$$

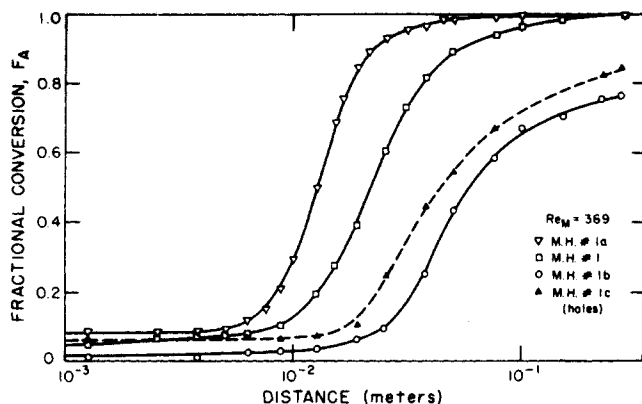


Figure 5a. Extent of reaction versus distance from mixing head with stoichiometric amounts of reagents and $Re_M = 369$ for mixing heads composed with circular tubes (Fisher, 1974).

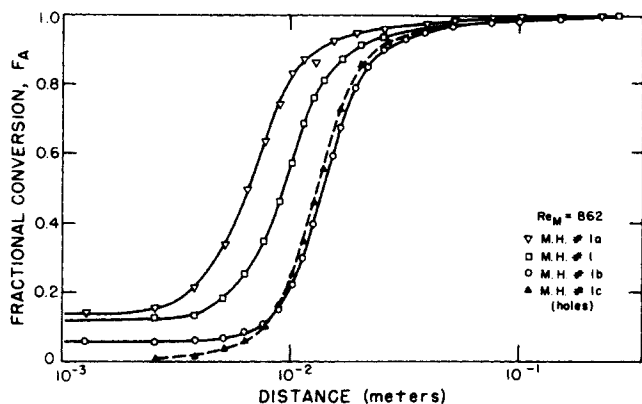


Figure 5b. Extent of reaction versus distance from mixing head with stoichiometric amounts of reagents and $Re_M = 862$ for mixing heads composed of circular tubes (Fisher, 1974).

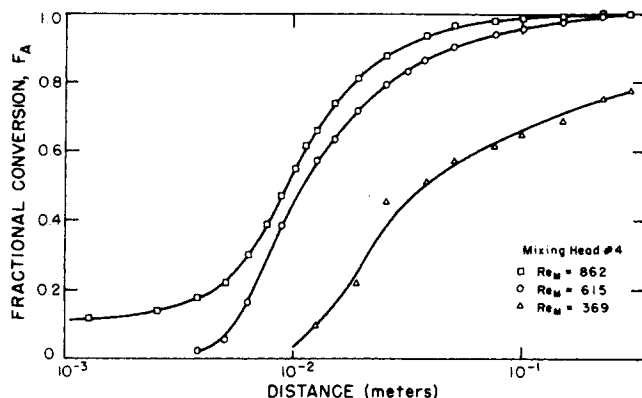


Figure 5c. Extent of reaction versus distance from mixing head with stoichiometric amounts of reagents for mixing head #4 at various Reynolds numbers (Fisher, 1974).

Exceptional care is required to obtain meaningful data. Eq. 4.1 holds only if there is neither appreciable heating from viscous dissipation of the turbulence nor heat diffusion. High thermal diffusivities will tend to produce flat temperature profiles. Ou (1980) has proved that under the experimental conditions this effect is negligible.

Although a number of different experiments were performed (Fisher, 1974), we restrict ourselves to those in which hydrochloric acid and sodium hydroxide solution were reacted while: (1) Reynolds number was changed by varying the flow rate; and (2) turbulence intensity was varied by changing the mixing head feeding the reactants.

A typical set of reaction results is shown in Figures 5a, b, c plotted as fractional conversion, F_A , versus log of the distance downstream from the mixing head, z . F_A did not approach zero

as z becomes very small since the region immediately downstream of the mixing head contained some recirculated fluid. Recirculation causes a nonuniform residence time distribution, especially apparent at small distances, and allows for some apparent reaction even as $z \rightarrow 0$. Results of Figures 5a, b, c are parameterized by a Reynolds number, defined as:

$$Re_M = \frac{UM\rho}{\mu} \quad (4.2)$$

where U is the mean velocity in the reactions and M is the periodicity of the grid (Fisher, 1974).

Multijet reactors can be considered to be continuous flow mixers, and Section 3 can be applied to analysis of reaction data. Quantitative results in terms of the Lamellar Mixing Model depend on knowledge of local fluid mechanics, that is, knowledge of the function $\alpha(X, t) = -D \cdot \nabla^2 \hat{n}$ (Eq. 2.1) for any S_X -element. Generally, a prediction of $\alpha(X, t)$ implies, except in very simple cases, solution of a complicated fluid mechanical problem. Nevertheless, some understanding of the nature of this function can be gained by analysis of a particular classification of flows. Two cases will be considered here: mix heads with parallel slits (A) and mix heads with perforated plates (B).

Near the flow inlets, in both cases, there are surfaces of discontinuity that can be viewed as vortex sheets. In A, vortex sheets are parallel and form intermittent parallel vortex lines, and an essential feature is the two-dimensionality produced by the way material is introduced. In B, vortex rings of size of the order of the holes are produced intermittently. It is well known that vortex sheets are unstable (Landau and Lifshitz, 1978, p. 114) and readily break down into large-scale eddies that eventually divide or stretch into smaller ones (small scale of turbulence) or unite to form larger ones. Some average knowledge about this complex process can be obtained from turbulence measurements. Batchelor and Townsend (1952) differentiate among three periods of decay of turbulence intensity downstream of a mix head: an initial period, a final period, and an intermediate period. During the initial period of decay, the turbulent energy obeys the simple empirical law:

$$\frac{U^2}{u'^2} = a \left(\frac{z}{M} - \frac{z_0}{M} \right) \quad (4.3)$$

where

- U = mean velocity
- u'^2 = mean square velocity fluctuations
- M = periodicity of the grid
- a = empirical constant characteristic of a particular grid shape
- z = axial distance downstream from the grid
- z_0 = axial position where u'^2 appears to have infinite value

Within the initial period the volumetric energy dissipation rate can be determined directly. The pressure profile is stabilized soon after the exit from the grid or mixing head. Thus, for isotropic turbulence conservation of total energy shows (Batchelor and Townsend, 1952):

$$\epsilon = -U \frac{3}{2} \rho \frac{du'^2}{dz} \quad (4.4)$$

Substituting Eq. 4.3 for u'^2

$$\epsilon = \frac{3}{2} \rho U^3 \frac{M}{a(z - z_0)^2} \quad (4.5)$$

In terms of apparent residence time:

$$\epsilon = \frac{3}{2} \rho U \frac{M}{a(t - t'_0)^2} \quad (4.6)$$

where $t'_0 = z_0/U$. Thus, Eq. 4.6 expresses volumetric energy dissipation as a function of experimental parameters and is valid

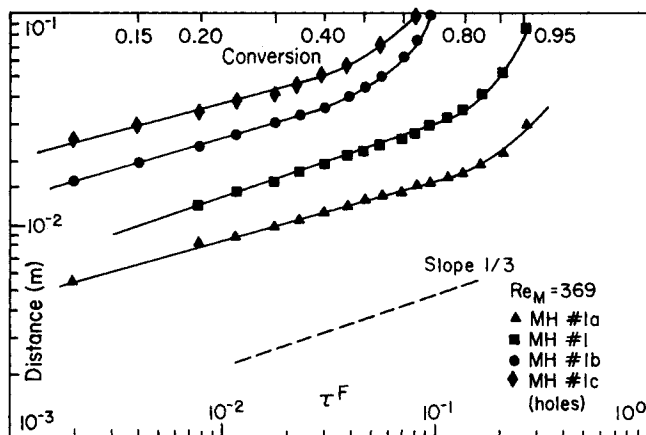


Figure 6a. Relation between real time t , and warped time, τ^F .

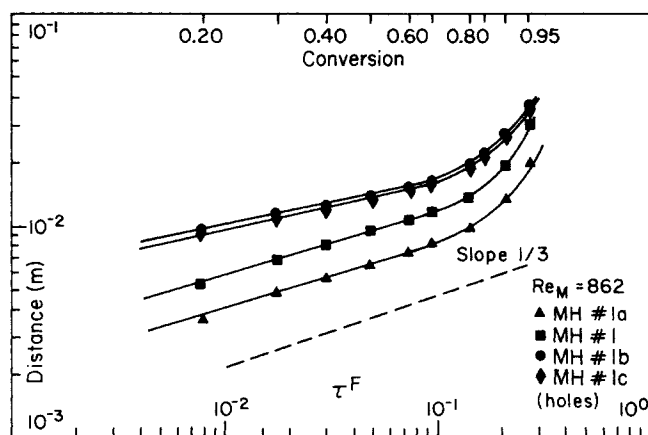


Figure 6b. Relation between real time t , and warped time, τ^F .

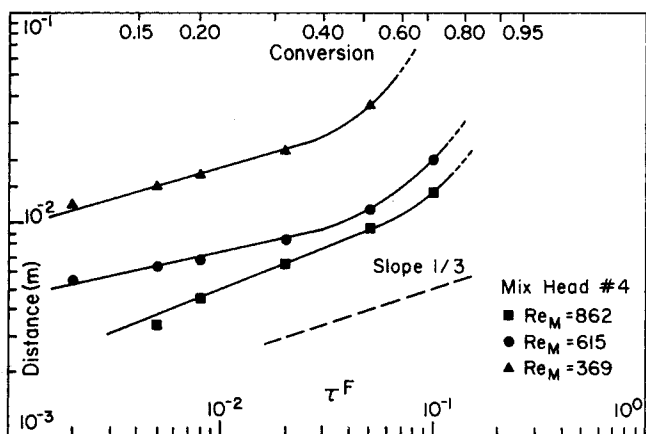


Figure 6c. Relation between real time t , and warped time, τ^F .

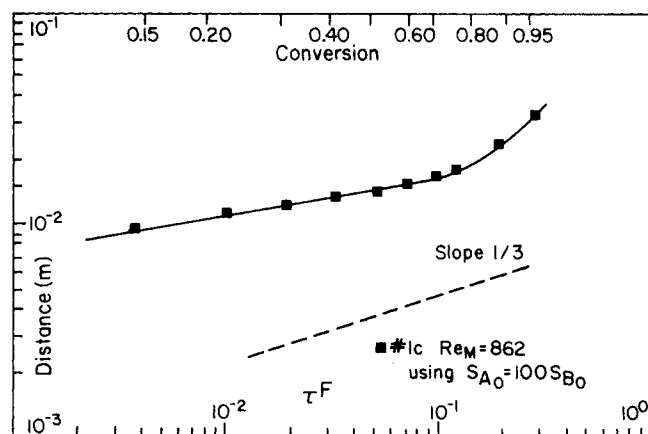


Figure 6d. Relation between real time t , and warped time, τ^F .

across any cross sectional area A perpendicular to the coordinate z .

Creation of intermaterial area is now given by Eq. 3.16 [defining $\overline{eff(t)}$] as:

$$\frac{d \langle \langle a_r \rangle \rangle}{\langle \langle a_r \rangle \rangle dt} \equiv \overline{eff(t)} \sqrt{\frac{3}{4}} \frac{Re_M}{a} \frac{1}{(t - t_0)} \quad (4.7)$$

since

$$\left(\frac{\bar{\epsilon}}{2\mu} \right)^{\frac{1}{2}} = \sqrt{\frac{3}{4}} \frac{Re_M}{a} \frac{1}{(t - t_0)} \quad (4.8)$$

and $dz/dt = \bar{v}_z$ or $\bar{v}_z = z/t$ for the plug flow in the tubular reactor. Furthermore, by flow radial independency $\langle \langle a_r \rangle \rangle = \bar{a}_r$ and Eq. 4.7 is written as:

$$\frac{d\bar{a}_r}{\bar{a}_r dt} \equiv \overline{eff(t)} \sqrt{\frac{3}{4}} \frac{Re_M}{a} \frac{1}{(t - t_0)} \quad (4.9)$$

which is in a convenient form for determining $\overline{eff(t)}$ from data analysis.

If at any particular cross sectional area A the real time associated with each S_x element is assumed to be the same, Eq. 3.14 becomes:

$$\tau = D \int_0^t \frac{1}{\bar{a}_r^2} dt' > D \int_0^t \frac{1}{\bar{a}_r'^2} dt' \quad (4.10)$$

There is, however, no guarantee about the closeness of \bar{a}_r^2 and $\bar{a}_r'^2$. A particular plane A will contain in general a distribution of

intermaterial area $\rho(a_r^2)$ such that $\int_0^\infty \rho(a_r^2) da_r^2 = 1$. Local chemical conversion presents a distribution over the plane A according to the local warped time distribution produced by intermaterial area variations. The mean area value of chemical conversion, which is the value assumed to be measured by the recording mechanisms, is calculated as $\overline{F(\tau)}$ and the value corresponding to the mean warped time is $F(\tau)$.

Convexity properties of the function $F(\tau)$ dictate useful inequalities. For the case 1 in Figure 2a the relation $F(\tau)$ is:

$$F = 1 - \frac{8}{\pi^2} \sum_{n=1,3,5}^{\infty} \frac{1}{n^2} \exp[-n^2 \pi^2 \tau] \quad (4.11)$$

and application of convexity properties (Hardy et al., 1973) shows, cf. Ottino (1980),

$$\int_0^\infty \rho(\tau) F(\tau) d\tau < F \left[\int_0^\infty \rho(\tau) \tau d\tau \right] \quad (4.12)$$

or

$$\overline{F(\tau)} < F(\tau) \quad (4.13)$$

Conversion at a particular plane calculated with the mean value of segregation results in over-estimation of actual mean conversion.

As explained in Section 3, the numerical results of the Laminar Mixing Model for Fast Reaction (Figures 2 and 3) are interpreted as $\bar{F}_A = \bar{F}_A(\tau)$; i.e., the model gives the average conver-

sion of an element experiencing the average warped time history.

The relation $\tau = \tau(t)$ is obtained by elimination of fractional conversion between Figure 2, curve 1, and Figures 5a, b, c. The results are shown in Figures 6a-d. The basic result is:

$$\frac{d \ln t}{d \ln \tau} \approx \frac{1}{3} \quad (4.14)$$

up to conversions of 80%, and²

$$\frac{d \ln t}{d \ln \tau} \geq \frac{1}{3} \quad (4.15)$$

for higher conversions. According to Section 3, Eq. 4.14 implies

$$\frac{d \bar{a}_r}{\bar{a}_r dt} \approx \overline{eff(t)} \sqrt{\frac{3}{4}} \frac{Re_M}{a} \frac{1}{(t - t_o)} = \frac{(3 - 1)}{2t} \quad (4.16)$$

and a constant efficiency parameter. A constant value of efficiency parameter implies an exponential increase of mean area of material planes as functions of time in material regions with uniform and constant viscous dissipation (cf., Eq. 3.16). Eq. 4.16 implies a linear time increase of mean intermaterial area increase downstream of the mixing head.

The result (Eq. 4.15) is consistent with the definition of efficiency index since it implies eventually decaying values as functions of distance downstream of the mixing head. It could well imply growing efficiencies that could reach and eventually surpass the value of one in contradiction to the definition of this parameter. The appearance of time decaying efficiencies can be proved by the following reasoning: for plug flow Eqns. 3.14 and 4.14 imply:

$$t \frac{d\tau}{dt} \leq 3\tau \quad (4.17)$$

and

$$D \bar{a}_r^2 t \leq 3\tau \quad (4.18)$$

Due to radial flow independency $d\tau/dt = D\bar{a}_r^2 = D\bar{a}_r^2$. "Inequality 4.18 can be shown to be compatible with:

$$\frac{d \bar{a}_r}{\bar{a}_r dt} = \overline{eff(t)} \sqrt{\frac{3}{4}} \frac{Re_M}{a} \frac{1}{(t - t_o)} \leq \frac{1}{t} \quad (4.19)$$

which shows that $\overline{eff(t)}$ in this system must eventually be a decaying function of time.³

An estimate of the intermaterial area values downstream of the mix head in the multijet reaction can be obtained by Eq. 3.15. Values calculated with this formula present a maximum intermaterial area of the order $\bar{a}_r = s^{-1} = 10^5 \text{ m}^2/\text{m}^3$. [These values are coincident with the segregation scale δ of Mao and Toor (1970). However, the parameter δ of Mao and Toor was a fitting parameter for which physical meaning is provided here.]

APPLICATION OF AN EFFICIENCY FUNCTION TO ANALYSIS OF MIXING IN STIRRED TANKS

Fisher (1974) also studied the reaction between hydrochloric acid and sodium hydroxide dissolved in an aqueous sugar solution in a centrally stirred tank reactor of standardized dimensions (Brown, 1950). Fractional average conversion was measured at a particular point in the reactor with the temperature rise technique of Vassilatos and Toor (1965), and direct measurements of power dissipation were made by torque meter over the range of Reynolds number encountered in the reaction

² In some other cases reported by Fisher deviations in the range 40-80% conversion were observed. The trend of Eqs. 4.15 and 4.19 was found in most cases.

³ Speculations can be offered to explain decaying efficiency functions. Finite thickness of reaction zone (Ranz, 1979), inappropriate use of Eq. 4.3, and long-range diffusion effects produced by local stoichiometry imbalance (Ottino, 1980) are possible explanations.

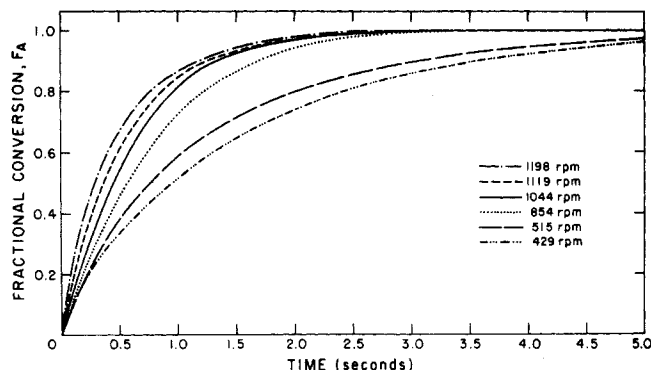


Figure 7. Extent of reaction versus time for several agitation rates in CSTR reactor (from Fisher, 1974).

experiments.⁴ Care was taken to provide consistent initial conditions for mechanical mixing. Reactants were separated by an elastic, *in-situ* formed, rubber membrane, and homogeneous and identical conditions were established in both phases previous to initiation of stirring.

Figure 7 shows average extent of reaction vs. time at various stirring speeds. For details the reader is referred to Fisher (1974).

The stirred tank can be considered to be a closed volume mixer and as such the analysis of Section 3 applies. For such systems mean volumetric intermaterial area follows the equation:

$$\frac{d \bar{a}_r}{\bar{a}_r dt} = \overline{eff(t)} (\overline{\tau \cdot D})^{\frac{1}{2}} \quad (5.1)$$

where $\overline{eff(t)}$ is an efficiency index of mixing always less than unity. For Newtonian fluid in terms of viscous dissipations per unit volume, $\overline{\tau \cdot D}$, Eq. 5.1 is written as:

$$\frac{d \bar{a}_r}{\bar{a}_r dt} = \overline{eff(t)} \left(\frac{\overline{\tau \cdot D}}{2\mu} \right)^{\frac{1}{2}} \quad (5.2)$$

The value of $\overline{\tau \cdot D}$ can be obtained with the viscous dissipation measurements. As indicated in Section 3, the Lagrangian information of the Lamellar Model can be interpreted as mean volumetric average conversion as function of real time, i.e., Figure 2 is interpreted as $F_A = F_A(\tau^F)$. Elimination of F_A between the model of Figure 2, curve 1 and the experimental data of Figure 7 produce the curves depicted in Figure 8. Two regimes of

$$\frac{d \ln \tau^F}{dt} = \text{const} \quad (5.3)$$

can be proposed, during periods 0.00-0.25 s and 1.5-3.5 s. These are regimes of nearly exponential mean intermaterial area growth. This is so, since Eq. 5.3 implies that (cf. Eq. 3.10).

$$\frac{d \bar{a}_r}{\bar{a}_r dt} = \frac{\text{const}}{2} = \overline{eff(t)} \left(\frac{\overline{\tau \cdot D}}{2\mu} \right)^{\frac{1}{2}} \quad (5.4)$$

All terms in Eq. 5.4 can be computed to calculate $\overline{eff(t)}$; const from Figure 8 and $\overline{\tau \cdot D}$ from power dissipation measurements. For 429 rpm, $\overline{eff(t)} = 0.338$ for $0 < t < 0.25$ s and $\overline{eff(t)} = 0.0136$ for $t > 1$ s. For 1198 rpm, $\overline{eff(t)} = 0.221$ for $0 < t < 0.25$ s and $\overline{eff(t)} = 0.0069$ for $t > 1$. Property values and reactor dimensions used in the calculations are:

⁴ Fisher's power measurements (Fisher, 1974) do not agree with published correlations for power dissipation in the standard configuration (Rushton et al., 1950). However measured energy dissipation, averaged over tank volume, will be used here for the value of $\overline{\tau \cdot D}$.

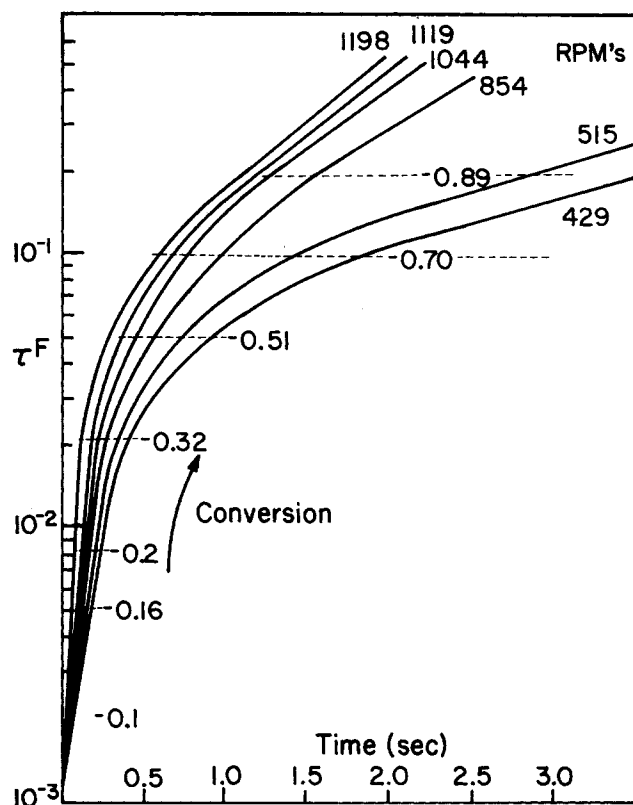


Figure 8. Relation between real time and warped time (τ^F) for the experimental data of Figure 7. Conversion F_A was converted to τ^F using curve 1 in Figure 2.

- ρ = density of the solution = $1.13 \times 10^3 \text{ kg/m}^3$
 μ = viscosity of the solution = $0.119 \text{ kg/m}\cdot\text{s}$
 D = tank diameter = 0.1252 m
 V = tank volume = $4.62 \times 10^{-3} \text{ m}^3$
 D_i = impeller diameter = $4.17 \times 10^{-2} \text{ m}$

High levels of agitation seem to be less efficient. This can be anticipated by the limiting profile in Figure 7. We note that the value of efficiency for long times is of the same order of magnitude as those reported for *viscous* mixing in stirred tanks (Ottino and Macosko, 1980). Also, note that this *turbulent* stirred tank is not really a volume of uniform turbulence in which the energy is put into well distributed large eddies, inside which are the smaller eddies, inside which are the smallest eddies where dissipation occurs. There is a well defined circulation into the top and bottom of the impellers and outward from the blades. This circulation is of time of order of 2 s. Thus in the beginning motion in the tank is more like a time decay of turbulence downstream from a mixing head (Section 4) than it is a volume of uniform turbulence. The high efficiency index-values for short times seem to confirm this interpretation.

ACKNOWLEDGMENT

The author is indebted to W. E. Ranz (University of Minnesota) for many discussions and comments during the execution of this work.

NOTATION

- a_v = intermaterial area per unit volume
 c_A, c_B = concentrations of A and B respectively
 D = diffusion coefficient
 \underline{D} = stretching tensor, $\frac{1}{2}[\nabla \underline{v} + (\nabla \underline{v})^T]$
 $\overline{eff}(z), \overline{eff}(t)$ = mixing efficiencies, dimensionless
 F_A, F_B = chemical conversion of A and B respectively
 k_2 = second order reaction constant

- \hat{n} = unit vector
 S_x = microflow element
 s = striation thickness
 t = time, t' and t'' variables of integration
 U = mean velocity in mix-head
 u' = velocity fluctuation
 v_n = normal component of the velocity vector to cross sectional area
 \underline{X} = Lagrangian coordinate, particle \underline{X}
 y = coordinate normal to intermaterial planes
 z = axial distance

Greek Letters

- $\alpha(\underline{X}, t)$ = stretching function
 ϵ = viscous dissipation per unit volume per unit time
 μ = viscosity
 ν = stoichiometric coefficient
 ξ = nondimensional distance in striation thickness based space
 ρ = density
 \underline{T} = viscous part of the stress tensor
 τ = warped time, dimensionless; τ^F warped time for fast reactions

Subscripts

- A, B = compounds A, B
 0 = initial value
 $'$ = fluctuation in local mean value

Special Symbols

- — = volume average
 $\langle\langle \rangle\rangle$ = mixed cup average
 — = area average

LITERATURE CITED

- Batchelor, G. K., and A. A. Townsend, "Turbulent Diffusion," *Surveys in Mechanics*, G. K. Batchelor and R. M. Davis, eds., Cambridge University Press (1952).
 Brodkey, R. S., "Fluid Motion and Mixing," *Mixing*, 1, V. H. Uhl and J. B. Gray, eds., Academic Press, New York (1966).
 Brown, G. G., *Unit Operations*, J. Wiley Inc., New York (1950).
 Fisher, D. A., "Development and Application of a Model for Fast Reactions in Turbulently Mixed Liquids," Ph.D. Thesis, University of Minnesota, Minneapolis, MN (1974).
 Hardy, G. H., J. E. Littlewood, and G. Pólya, *Inequalities*, 2nd ed., Cambridge University Press (1973).
 Landau, L. D., and E. H. Lifshitz, *Fluid Mechanics*, Pergamon Press, Elmsford, NY (1978).
 Mao, K. W., and H. L. Toor, "A Diffusion Model for Fast Reactions with Turbulent Mixing," *AIChE J.*, **16**, 49 (1970).
 Ottino, J. M., W. E. Ranz, and C. W. Macosko, "A Lamellar Model for Analysis of Liquid-Liquid Mixing," *Chem. Eng. Sci.*, **34**, 877 (1979).
 Ottino, J. M., "Lamellar Mixing Models for Structured Chemical Reactions and Their Relationship to Statistical Models; Macro- and Micro-Mixing and the Problem of Averages," *Chem. Eng. Sci.*, **35**, 1377 (1980).
 Ottino, J. M., and C. W. Macosko, "An Efficiency Parameter for Batch Mixing of Viscous Liquid," *Chem. Eng. Sci.*, **35**, 1454 (1980).
 Ou, J. J., "Mixing and Chemical Reactions," Ph.D. Thesis, University of Minnesota, Minneapolis, MN (1980).
 Ranz, W. E., "Applications of a Stretch Model to Mixing, Diffusion, and Reaction in Laminar and Turbulent Flows," *AIChE J.*, **25**, 41 (1979).
 Rushton, J. H., E. W. Costech, and H. J. Everett, "Power Characteristics of Mixing Impellers. Part II," *Chem. Eng. Prog.*, **46**, 467 (1950).
 Vassiliatos, G., and H. L. Toor, "Second-Order Chemical Reactions in a Nonhomogeneous Turbulent Fluid," *AIChE J.*, **11**, 666 (1965).

Manuscript received November 15, 1979; revision received May 23, and accepted July 9, 1980.